IEEE Access
Multidisciplinary ⋮ Rapid Review ⋮ Open Access Journal

Received August 29, 2017, accepted September 20, 2017, date of publication October 9, 2017, date of current version October 25, 2017.

Digital Object Identifier 10.1109/ACCESS.2017.2758377

A Semi-Supervision Fault Diagnosis Method Based on Attitude Information for a Satellite

ZHIQIANG ZHANG, ZHIYONG SHE, AND AIHUA ZHANG, (Member, IEEE)
College of Engineering, Jinzhou 121013, China

Corresponding author: Zhiqiang Zhang (jsxinxi_zzq@163.com)

This work was supported in part by the National Natural Science Foundation of China under Project 61603056, in part by the National Natural Science Foundation of Liaoning under Project 2015020042, and in part by the Excellent Talents to Support Projects In Liaoning Province of China under Project LJQ2015003.

ABSTRACT The various faults that inevitably occur represent a primary issue in satellite on-orbit operation. Fault diagnosis is the first step in the fault control process. As a means to perform this step, a semi-supervision fault diagnosis method via attitude information is proposed for a satellite. This method combines static fusion with dynamic updating. The evidence concept is employed to obtain the fault information. It not only allows the detection of the slow change and failure with interference, but also confirms the optimal fusion and updating parameters via historical data. Numerical simulations, including static fusion diagnosis and dynamic updating diagnosis, are all presented with the proposed semi-supervision diagnosis methods to compare and prove the effectiveness of the proposed approach.

INDEX TERMS Fault diagnosis, semi-supervision, static fusion, dynamic updating, satellite.

I. INTRODUCTION

Satellites, in the future, will be expected to achieve highly accurate pointing and fast slewing in the practical environment. However, various faults are inevitably faced during the time a satellite is in orbit. If this problem cannot be solved, then the occurrences of these faults will deteriorate the control behavior. Therefore, satellite attitude control systems with high performance design should consider various faults; in particular, actuator faults must be taken into account.

A fault is defined as an unpermitted deviation of at least one characteristic property or parameter of the system from the acceptable condition [1]. Usually, fault diagnosis includes fault detection, fault isolation and fault identification. Fault detection could determine quickly if the system or component acts abnormally. Fault isolation could isolate the point or component that has caused the fault. In addition, fault identification could confirm the fault type and degree of severity of the system status. Fault tolerance control is an advanced control approach. Most fault tolerance systems, which have widespread industrial applications, use fault diagnosis system/fault isolation/fault identification. The purpose of these systems is to guarantee that the system has immunity to faults or achieves acceptable control performance after the occurrence of various faults. Usually, fault diagnosis and fault tolerance control are integrated. To facilitate the detailed expression of the fault tolerance approach, a simplified schematic is presented in Fig. 1 [2].

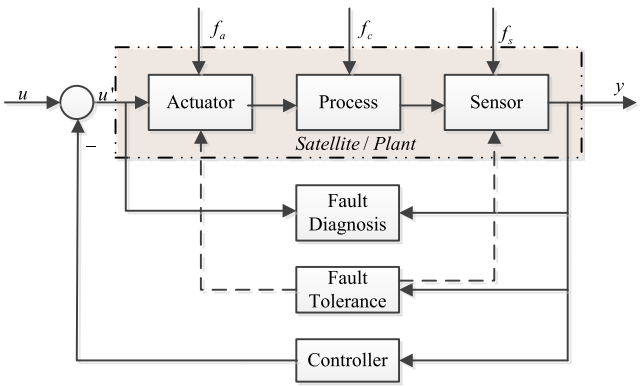

FIGURE 1. Simplified schematic of the fault tolerance approach.

In the figure, $\boldsymbol{u}$ is the reference input vector, $\boldsymbol{u}'$ is the control input vector, $\boldsymbol{y}$ is the measured output vector, $\boldsymbol{f_a}$ is the actuator fault, $\boldsymbol{f_c}$ is the parameter fault and $\boldsymbol{f_s}$ is the sensor fault. The purpose of fault diagnosis technology is to monitor real-time and diagnose the system status (whether there is a fault, the fault position and the fault case.)

During the past four decades, many fault diagnosis approaches and their applications in various industrial control fields have been reported. The detailed comprehensive

analysis presented in [2] and [3] introduced the following three concepts of fault diagnosis: 1) model-based fault detection and diagnosis, 2) observer-based methods, and 3) parameter estimation techniques [4]–[9]. Many technologies have been employed in this field, such as adaptive control [10], [11] and slide mode control [12], [13]. Subsequently, many quantitative mode-based, qualitative model based and research strategies, and process history-based methods were proposed [14]–[16]. Afterwards, pattern recognition technology was developed. 1-class support vector machine (SVM) is a special variant of the general SVM; because only the normal data is required for training, 1-class SVM is widely used in anomaly detection [17]. Based on the above references, a robust 1-class SVM was proposed [18]. With the designed penalty factors, the robust 1-class SVM can not only diagnose the fault accurately but also depress the influences of outliers. Standard partial least squares serves as a powerful tool for monitoring key performance indicators in the large-scale process industry [19]. Subsequently, an improved partial least squares approach was presented in [20]. This method can decompose the measurable process variables into the KPI-related and unrelated parts. Similar issues are discussed in [21]. Application of data-driven technology in the fault diagnosis field began from [22]–[24]. Some refer to this technology as real active fault diagnosis. Subsequently, implementation of similar technology became popular. Wang *et al.* [25] proposed a data-driven method for the task of fault detection in nonlinear systems. This method employed the locally weighted projection regression to serve as a powerful tool for modeling the nonlinear process with locally linear models. In addition, partial least squares regression is performed for each local model. A partial least square (PLS) based fault detection scheme is applied to monitor the regional model. Yin *et al.* [24] provided an overview of the recent developments in data-based techniques focused on modern industrial applications. As one of the most popular research topics for complicated processes, data-based techniques have been rapidly developed over the past two decades and are currently widely used in numerous industrial sectors. Fault diagnosis is essential to the field. To address the demands of real-time fault diagnosis, the supervision fault diagnosis system was developed [26]. The supervision system performs fault detection and diagnosis. Based on the appropriate detection or diagnosis results, the corresponding fault tolerance controller can be designed. However, the supervision fault diagnosis is based on known fault information; if an unknown fault occurs, then the diagnosis is uncertain. Thus, the no-supervised idea is employed. Many researchers put their eyes on the topic of unsupervised. In the recent [27], it presents an unsupervised learning method to predict noise. And [28] discusses the advantage and defect of semi-supervised and unsupervised learning method.

In this paper, a semi-supervision fault diagnosis method based on attitude information for a satellite is developed. Static fusion and dynamic updating evidence concepts are separately employed. Considering the demands of real-time operation, the semi-supervision fault diagnosis combines static fusion with dynamic updating. Moreover, the evidence concept is employed to show the fault diagnosis information. It not only detects slow change and failure with interference but also confirms optimal fusion and updated parameters via the historical data.

The remainder of this paper is organized as follows. Section II presents preparations. Section III presents a detailed introduction of the semi-supervision fault diagnosis method based on attitude information for a satellite. Simulation results to demonstrate various features of the proposed scheme are given in Section IV. The conclusions are presented in Section V.

II. PREPARATIONS

A. SATELLITE MATHEMATICAL MODEL

The attitude kinematics and dynamics of a satellite are obtained from [29]:

$$\begin{cases} \dot{\boldsymbol{q}} = \dfrac{1}{2}(\boldsymbol{q}^{\times} + q_0 \boldsymbol{I}_3)\boldsymbol{\omega} \\ q_0 = -\dfrac{1}{2}\boldsymbol{q}^T \boldsymbol{\omega} \\ \boldsymbol{J}\dot{\boldsymbol{\omega}} + \boldsymbol{\omega}^{\times}\boldsymbol{J}\boldsymbol{\omega} = \boldsymbol{u} + \boldsymbol{d} \end{cases} \tag{1}$$

where $\boldsymbol{\omega} = [\boldsymbol{\omega}_1, \boldsymbol{\omega}_2, \boldsymbol{\omega}_3]^T$ denotes the angular velocity of the spacecraft expressed in the body-fixed frame, $\boldsymbol{q} = \begin{bmatrix} q_1 & q_2 & q_3 \end{bmatrix}^T$, q_0 denotes the unit quaternion representing the attitude orientation of the satellite between the body-fixed frame and the inertial frame, $\boldsymbol{I}_3$ denotes the identity matrix of three orders, $\boldsymbol{u}$ is the total control torque acting on the satellite, $\boldsymbol{d}$ denotes the external disturbances, and the operator $\boldsymbol{q}^{\times}$ denotes the skew-symmetric matrix given by

$$\boldsymbol{q}^{\times} = \begin{bmatrix} 0 & -q_3 & q_2 \\ q_3 & 0 & -q_1 \\ q_2 & \omega_1 & 0 \end{bmatrix} \tag{2}$$

Assumption 1: The disturbance $\boldsymbol{d}$ is bounded, and there is a positive scalar $d_{\max}$ that satisfies $||\boldsymbol{d}|| \leq d_{\max}$.

For any on-orbit satellite, gravity-gradient torque, aerodynamic torque, solar radiation torque, and earth magnetic torque are the primary external disturbances for $\boldsymbol{d}$ in Eq.(1) [30]. Those disturbances are bounded in practice. Therefore, Assumption 1 is reasonable. In fact, as given in [30], the upper bound $d_{\max}$ can be conservatively calculated.

B. ACTUATOR FAULTS

The satellite considered in this work is controlled using reaction wheels.

Assume that three reaction wheels are mounted in the satellite. For the i^{th} actuator, $i = 1, 2, 3$, whose configuration is shown in Fig. 2, the force component can be derived as

$$\boldsymbol{F}_i = F_i \begin{bmatrix} \cos\alpha_i \cos\beta_i \\ \cos\alpha_i \sin\beta_i \\ \sin\alpha_i \end{bmatrix} \tag{3}$$

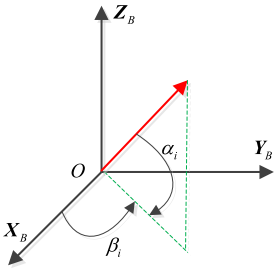

FIGURE 2. Actuator azimuth and elevation.

where $F_i > 0$ is the constant thrust level, α_i is the elevation angle, and β_i is the azimuth angle. Let $\boldsymbol{r}_i = r_{xi}\boldsymbol{X}_B + r_{yi}\boldsymbol{Y}_B + r_{zi}\boldsymbol{Z}_B$ be the vector representing the placement of the actuator from the satellite center of mass. The torque component provided by the i^{th} actuator can be calculated as

$$\boldsymbol{\tau}_i = \boldsymbol{r}_i \times \boldsymbol{F}_i \tag{4}$$

Next, the applied control torque $\boldsymbol{u}$ generated by three reaction wheels is

$$\boldsymbol{u} = \sum_{i=1}^{N} \boldsymbol{\tau}_i = \sum_{i=1}^{N} \boldsymbol{r}_i \times \boldsymbol{F}_i \tag{5}$$

In this study, actuator faults, including misalignment error and theirs magnitude error, are considered. The nature of those two scenarios is described as follows:

1) MISALIGNMENT ERROR

The configuration of actuators is not perfect in practice. Misalignment error may occur because of space debris or the limitations of the manufacturing technique used. The demanded torque from the controller is thus different from the torque produced by the actuators. For reaction wheels, misalignment error may exist in $\boldsymbol{r}_i$ and the alignment angles α_i & β_i. Let $\boldsymbol{r}_i^n$ and $\Delta\boldsymbol{r}_i$ denote the nominal and the alignment error distance, respectively, between satellite center and the actuators. Thus, $\boldsymbol{r}_i$ can be rewritten as $\boldsymbol{r}_i = \boldsymbol{r}_i^n + \Delta\boldsymbol{r}_i$. Suppose that the actuator is titled over a nominal direction with small constant angles, $\Delta\alpha_i$ and $\Delta\beta_i$. Thus, the alignment angle can be denoted as $\alpha_i = \alpha_i^n + \Delta\alpha_i$ and $\beta_i = \beta_i^n + \Delta\beta_i$, where α_i^n and β_i^n are the nominal alignment angles.

2) ACTUATOR MAGNITUDE ERROR

As discussed in [31], let F_n and ΔF_i represent the nominal and error of the actuator magnitude, respectively. The actual actuator F_i can thus be denoted by

$$F_i = F_n + \Delta F_i \tag{6}$$

Because of the physical limitation of the actuator, the actual actuator F_i generated is not negative, and its maximum actuator should be less than F_n, *i.e.*, $0 \le F_i \le F_n$. Hence, the error of actuator magnitude ΔF_i is such that $-F_n \le \Delta F_i \le 0$. The case of $\Delta F_i = 0$ corresponds to the i^{th} actuator operating normally. The case of $\Delta F_i = -F_n$ corresponds to the i^{th} actuator being completely lost. The case of $-F_n < \Delta F_i < 0$ corresponds to the i^{th} actuator partially losing its effectiveness because of reduction in the amount of a propellant's mass and low pressure of the tank.

Taking actuator faults into consideration, $\boldsymbol{\tau}_i$ in (4) can be rewritten as

$$\begin{aligned}\boldsymbol{\tau}_i &= (F_n + \Delta F_i)(\boldsymbol{r}_i^n + \Delta\boldsymbol{r}_i) \\ &\quad \times \begin{bmatrix} \cos(\alpha_i^n + \Delta\alpha_i)\cos(\beta_i^n + \Delta\beta_i) \\ \cos(\alpha_i^n + \Delta\alpha_i)\sin(\beta_i^n + \Delta\beta_i) \\ \sin(\alpha_i^n + \Delta\alpha_i) \end{bmatrix} \\ &= F_n(\boldsymbol{r}_i^n) \times \boldsymbol{D}_i^n + \Delta F(\boldsymbol{r}_i^n) \times \boldsymbol{D}_i^n + (F_n + \Delta F_i)[(\boldsymbol{r}_i^n) \\ &\quad \times \Delta\boldsymbol{D}_i^n + \Delta\boldsymbol{r}_i \times (\boldsymbol{D}_i^n + \Delta\boldsymbol{D}_i^n)]\end{aligned} \tag{7}$$

where

$$\boldsymbol{D}_i^n = \begin{bmatrix} \cos\alpha_i^n \cos\beta_i^n \\ \cos\alpha_i^n \sin\beta_i^n \\ \sin\alpha_i^n \end{bmatrix}$$

$$\Delta\boldsymbol{D}_i^n = \begin{bmatrix} \cos(\alpha_i^n + \Delta\alpha_i)\cos(\beta_i^n + \Delta\beta_i) \\ \cos(\alpha_i^n + \Delta\alpha_i)\sin(\beta_i^n + \Delta\beta_i) \\ \sin(\alpha_i^n + \Delta\alpha_i) \end{bmatrix} \tag{8}$$

$$- \begin{bmatrix} \cos\alpha_i^n \cos\beta_i^n \\ \cos\alpha_i^n \sin\beta_i^n \\ \sin\alpha_i^n \end{bmatrix} \tag{9}$$

From (5) and (7), the real/total actuator force with magnitude error and misalignment is expressed as the sum of the nominal and thrust error terms in the body frame (10), as shown at the bottom of this page, where $\boldsymbol{u}_n \in \Re^3$ is the nominal control torque commanded by the controller and $\boldsymbol{u}_f \in \Re^3$ denotes the faulty torque induced by misalignment error and actuator magnitude error.

Assumption 2: The faulty torque $\boldsymbol{u}_f$ introduced by actuator faults is bounded by a positive scalar $u_{\max}$, *i.e.*, $||\boldsymbol{u}_f|| \le u_{\max}$.

Remark 2: Because of the physical limitation of the actuator, $|\Delta F_i| \le F_n$. Although the manufacturing technique is limited in precision, the inequality $||\Delta\boldsymbol{r}_i|| \le ||\boldsymbol{r}_i^n||$ can always be guaranteed. Hence, it follows that

$$\begin{aligned}||\boldsymbol{u}_f|| \le F_n \sum_{i=1}^{N} [&||(\boldsymbol{r}_i^n) \times \boldsymbol{D}_i^n|| + 2||(\boldsymbol{r}_i^n) \times \Delta\boldsymbol{D}_i^n \\ &+ \Delta\boldsymbol{r}_i \times (\boldsymbol{D}_i^n + \Delta\boldsymbol{D}_i^n)||]\end{aligned} \tag{11}$$

$$\boldsymbol{u} = \underbrace{F_n \sum_{i=1}^{N} (\boldsymbol{r}_i^n) \times \boldsymbol{D}_i^n}_{u_n} + \underbrace{\sum_{i=1}^{N} \{\Delta F(r_i^n) \times \boldsymbol{D}_i^n + (F_n + \Delta F_i)[(\boldsymbol{r}_i^n) \times \Delta\boldsymbol{D}_i^n + \Delta\boldsymbol{r}_i \times (\boldsymbol{D}_i^n + \Delta\boldsymbol{D}_i^n)]\}}_{u_f} \tag{10}$$

Moreover, it can be obtained from (9) that $||\Delta \boldsymbol{D}_i^n|| \leq 2\sqrt{3}$. Hence, (11) becomes

$$||\boldsymbol{u}_f|| \leq F_n \sum_{i=1}^{N} \{||(\boldsymbol{r}_i^n) \times \boldsymbol{D}_i^n|| + 2[2\sqrt{3}||\boldsymbol{r}_i^n|| + ||\boldsymbol{r}_i^n||||\boldsymbol{D}_i^n + 2\sqrt{3}||]\} \quad (12)$$

From (12), Assumption 2 is therefore reasonable because $\boldsymbol{u}_f$ is bounded by (12) at most.

Assumption 2: The faulty torque $\boldsymbol{u}_f$ introduced by actuator faults is bounded by a positive scalar $u_{\max}$, *i.e.*, $||\boldsymbol{u}_f|| \leq u_{\max}$.

Remark 1: Because of the physical limitation of the actuator, $|\Delta F_i| \leq F_n$. Although the manufacturing technique is limited in precision, the inequality $||\Delta \boldsymbol{r}_i|| \leq ||\boldsymbol{r}_i^n||$ can always be guaranteed. Hence, it follows that

$$\begin{aligned} ||\boldsymbol{u}_f|| &\leq \sum_{i=1}^{N} ||\Delta F(\boldsymbol{D}_i^n) \times \boldsymbol{D}_i^n + (F_n + \Delta F_i)[(\boldsymbol{D}_i^n) \times \Delta \boldsymbol{D}_i^n \\ &\quad + \Delta \boldsymbol{D}_i \times (\boldsymbol{D}_i^n + \Delta \boldsymbol{D}_i^n)]|| \\ &\leq F_n \sum_{i=1}^{N} [||(\boldsymbol{D}_i^n) \times \boldsymbol{D}_i^n|| + 2||(\boldsymbol{D}_i^n) \times \Delta \boldsymbol{D}_i^n \\ &\quad + \Delta \boldsymbol{D}_i \times (\boldsymbol{D}_i^n + \Delta \boldsymbol{D}_i^n)||] \end{aligned} \quad (13)$$

Moreover, it can be obtained from (9) that $||\Delta \boldsymbol{D}_i^n|| \leq 2\sqrt{3}$. Hence, (11) becomes

$$||\boldsymbol{u}_f|| \leq F_n \sum_{i=1}^{N} |\{|(\boldsymbol{r}_i^n) \times \boldsymbol{D}_i^n|| + 2[2\sqrt{3}||\boldsymbol{r}_i^n|| + ||\boldsymbol{r}_i^n||||\boldsymbol{D}_i^n + 2\sqrt{3}||]\} \quad (14)$$

From (12), Assumption 2 is therefore reasonable because u_f is bounded by (12) at most.

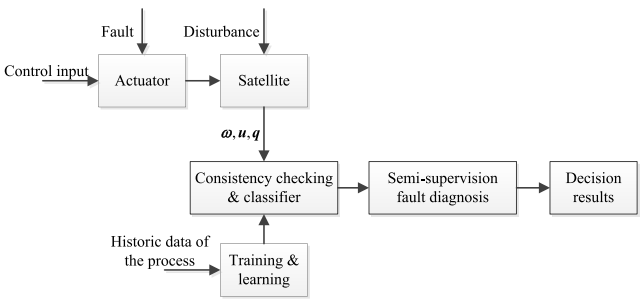

FIGURE 3. Schematic of the fault diagnosis for the actuator of a satellite.

III. A SEMI-SUPERVISION FAULT DIAGNOSIS METHOD BASED ON ATTITUDE INFORMATION FOR A SATELLITE

For convenient to understand the proposed fault diagnosis approach, here, a schematic of the fault diagnosis for the actuator of a satellite, shown in Fig. 3, is presented first.

In this paper, a semi-supervision fault diagnosis method is proposed to obtain fault information based on satellite attitude information. For realizing the semi-supervision fault diagnosis process, fusion and dynamic updating of diagnosis evidence is employed here. The process of the semi-supervision fault diagnosis based static fusion and dynamic updating, comes from [32], is shown in Fig. 4.

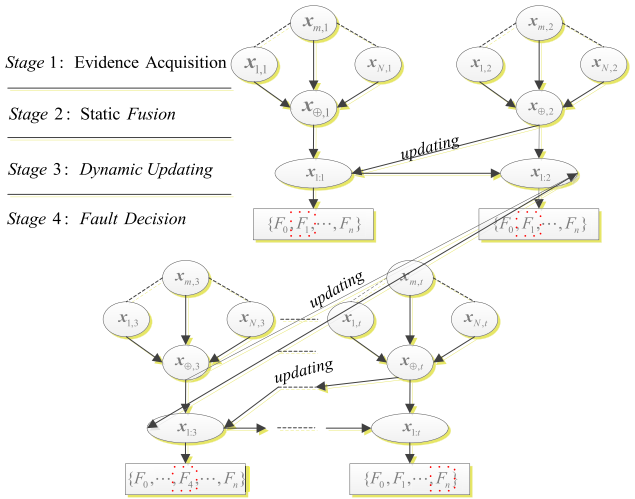

FIGURE 4. The process of the semi-supervision fault diagnosis.

A. THE PROCESS OF THE FAULT DIAGNOSIS INCLUDES FOUR STAGES

Stage 1 is the evidence acquisition stage. The local pieces of evidence are defined by $\boldsymbol{x}_{\boldsymbol{m},\boldsymbol{t}}$ $\boldsymbol{t} = \boldsymbol{1}, \boldsymbol{2}, \cdots, \boldsymbol{t}$, $\boldsymbol{m} = \boldsymbol{1}, \boldsymbol{2}, \cdots, \boldsymbol{N}$, where $\boldsymbol{m}$ is the number of the different sensors corresponding to $\boldsymbol{q}$, $\boldsymbol{\omega}$, $\boldsymbol{u}$ that can be obtained at every sampling instant $\boldsymbol{t}$.

Stage 2 is the static fusion stage. At time $\boldsymbol{t}$, the static fusion pieces of evidence $\boldsymbol{x}_{\oplus,\boldsymbol{t}}$ can be confirmed by fusing N $\boldsymbol{x}_{\boldsymbol{m},\boldsymbol{t}}$ according to the Dempster rule.

Stage 3 is the dynamic updating stage. The static fusion pieces of evidence $\boldsymbol{x}_{\oplus,\boldsymbol{t}}$ can be iterated and dynamically updated, and $\boldsymbol{x}_{\boldsymbol{1:t}}$ is defined as the updated pieces of evidence. Note that all the diagnosis information include the period of time from 1 to $\boldsymbol{t}$.

Stage 4 is the fault diagnosis decision stage. Both the reliability of the static pieces of evidence $\boldsymbol{x}_{\boldsymbol{m},\boldsymbol{t}}$ and dynamic updating of the pieces of evidence $\boldsymbol{x}_{\boldsymbol{1:t}}$ and the relation of the combination weight $\{\boldsymbol{\tau_t}, \boldsymbol{\nu_t}\}$ are considered. The evaluation function is defined to measure the reliability of $\boldsymbol{x}_{\boldsymbol{m},\boldsymbol{t}}$, $\boldsymbol{x}_{\boldsymbol{1:t}}$. In addition, based on the history sample data, the method of the discount rate $\alpha_{\boldsymbol{m}}$ and updating combination weight $\{\boldsymbol{\tau_t}, \boldsymbol{\nu_t}\}$ of the evidence are provided by optimized sensor $\boldsymbol{m}$. The detailed analysis can be found in [32]. The semi-supervision fault diagnosis method is proposed based on this reference. The following part will present the three stages of the semi-supervision fault diagnosis method, which includes static fusion, dynamic updating and fault diagnosis.

B. STATIC FUSION

First, we define $\boldsymbol{\Theta} = \{\boldsymbol{F_0}, \boldsymbol{F_1}, \cdots, \boldsymbol{F_n}\}$ to be the diagnosis frame and define $\boldsymbol{x}_{\boldsymbol{m},\boldsymbol{t}}^{\boldsymbol{\Theta}}$ or $\boldsymbol{x}_{\boldsymbol{m},\boldsymbol{t}}$ to be the diagnosis evidence of

the sensor $\boldsymbol{S_p}$. We define the discount rate variable to be $\boldsymbol{\alpha_m} = (\boldsymbol{\alpha_{1,m}}, \boldsymbol{\alpha_{2,m}}, \cdots, \boldsymbol{\alpha_{n,m}})$. The evidence ${}^{\boldsymbol{\alpha_m}}\boldsymbol{x_{m,t}}$ after discount of $\boldsymbol{\alpha_m}$ can be described by Mercier *et al.* [33],

$$ {}^{\alpha}x_S^{\Theta}(A) = \sum_{B\subseteq\Theta} {}^{\alpha}G(A,B)^{\alpha}x_S^{\Theta}(B), \quad \forall A \subseteq \Theta \tag{15} $$

Consider the Demspter [34] rule of composition,

$$ x(A) = \begin{cases} 1 - \dfrac{\sum\limits_{B\cap C=A} x_1(B)x_2(C)}{\sum\limits_{B\cap C=\emptyset} x_1(B)x_2(C)}, & A \neq \emptyset \\ 0, & A = \emptyset \end{cases} \tag{16} $$

If we fuse N pieces of evidence provided by the sensors via Eq.(16), then the static fusion result is

$$ {}^{\alpha}x_{\oplus,t} = {}^{\alpha_1}x_{1,t} \oplus + \cdots \oplus {}^{\alpha_m}x_{m,t} \oplus + \cdots \oplus {}^{\alpha_N}x_{N,t} \tag{17} $$

where $\alpha = (\alpha_1, \cdots, \alpha_m, \cdots, \alpha_N)$, and $\oplus$ expresses the Dempster combination operator.

To obtain the optimal solution, the evidence reliability static convergence objective function can be defined by

$$ \begin{aligned} &SI_m(\alpha_1, \cdots, \alpha_m, \cdots, \alpha_N) \\ &= \omega_{F0}\sum_{t=1}^{T_0} d^2({}^{\alpha}x_{\oplus,t}, x_{F_0}) + \omega_{F1}\sum_{t=1}^{T_1} d^2({}^{\alpha}x_{\oplus,t}, x_{F_1}) \\ &\quad + \cdots + \omega_{Fn}\sum_{t=1}^{T_n} d^2({}^{\alpha}x_{\oplus,t}, x_{F_n}) \end{aligned} \tag{18} $$

Eq.(18) is obtained from [33]. Next, the following optimization model can be employed to obtain the optimal solution of $(\alpha_1, \cdots, \alpha_m, \cdots, \alpha_N)$, which can guarantee $SI_m(\alpha_1, \cdots, \alpha_m, \cdots, \alpha_N)$ to be at its minimum, that is,

$$ \begin{aligned} &\min_{(\alpha_1,\cdots,\alpha_m,\cdots,\alpha_N)} SI_m(\alpha_1, \cdots, \alpha_m, \cdots, \alpha_N), \\ &s.t.\ 0 \le \alpha_{i,m} \le 1, \quad i = 1, 2, \cdots, N;\ m = 1, 2, \cdots, N \end{aligned} \tag{19} $$

C. DYNAMIC UPDATING

1) EVIDENCE OBTAINED

Based on [35], the evidence updating rule of conditional linear combination is defined by

$$ m_A(B) = \tau_A m(B) + v_A m(B|A) \tag{20} $$

Thus, the global evidence after updating can be solved by

$$ \begin{aligned} m_{1:t}(B) &= \tau_A m_{1:t-1}(B) + v_A m(B|D), \\ &B, D = F_0, F_1, \cdots, F_n, \Theta \end{aligned} \tag{21} $$

Suppose there are T pieces of evidence under the identification frame Θ. If the T pieces of evidence are marked with $m_1, m_2, \cdots, \cdots, m_T$, then the support degree function, supported $m_t, t = 1, 2, \cdots, T$ by the other $T-1$ evidence, according to [36], is

$$ Sup(m_t) = \sum_{\substack{q=1 \\ q\neq t}}^{T} Sim(m_t, m_q) \tag{22} $$

In addition, the credit of m_t is defined by [36]

$$ Crd(m_t) = \frac{Sup(m_t)}{\sum\limits_{t=1}^{T} Sup(m_t)} \tag{23} $$

$Crd(m_t)$ is the most relative importance weight reflecting the evidence.

According Eq.(21), the updated result ${}^{\alpha}x_{1:t-1}$ corresponding to time $t-1$ can be deduced, and the static fusion evidence ${}^{\alpha}x_{\oplus,t}$ and ${}^{\alpha}x_{\oplus,t+1}$, corresponding to times t and $t+1$, respectively, are confirmed. Therefore, the weight parameters can be obtained by the following Steps 1-3.

Step 1: Use strictly monotone decreasing similarity function

$$ Sim(x_1, x_2) = f(d(x_1, x_2)) = \frac{1}{1 + \exp(-a(0.5 - d(x_1, x_2)))} \tag{24} $$

to calculate between each pairing of ${}^{\alpha}x_{1:t-1}$, ${}^{\alpha}x_{\oplus,t}$ and ${}^{\alpha}x_{\oplus,t+1}$ as follows:

$$ \begin{aligned} &Sim(x_{1,t-1}, {}^{\alpha}x_{\oplus,t}) \\ &= \frac{1}{1 + \exp(-a(0.5 - d(x_{1,t-1}, {}^{\alpha}x_{\oplus,t})))} \end{aligned} \tag{25} $$

$$ \begin{aligned} &Sim(x_{1,t-1}, {}^{\alpha}x_{\oplus,t+1}) \\ &= \frac{1}{1 + \exp(-a(0.5 - d(x_{1,t-1}, {}^{\alpha}x_{\oplus,t+1})))} \end{aligned} \tag{26} $$

$$ \begin{aligned} &Sim({}^{\alpha}x_{\oplus,t}, {}^{\alpha}x_{\oplus,t+1}) \\ &= \frac{1}{1 + \exp(-a(0.5 - d({}^{\alpha}x_{\oplus,t}, {}^{\alpha}x_{\oplus,t+1})))} \end{aligned} \tag{27} $$

Step 2: Calculate the respective reliability of ${}^{\alpha}x_{1:t-1}$, ${}^{\alpha}x_{\oplus,t}$ and ${}^{\alpha}x_{\oplus,t+1}$ via Eqs.(22)-(23).

$$ Crd(m_{1:t-1}) = \frac{Sup({}^{\alpha}x_{\oplus,t-1})}{Sup(m_{1:t-1}) + Sup({}^{\alpha}x_{\oplus,t}) + Sup({}^{\alpha}x_{\oplus,t+1})} \tag{28} $$

$$ Crd(m_{1:t}) = \frac{Sup({}^{\alpha}x_{\oplus,t})}{Sup(m_{1:t-1}) + Sup({}^{\alpha}x_{\oplus,t}) + Sup({}^{\alpha}x_{\oplus,t+1})} \tag{29} $$

$$ Crd(m_{1:t+1}) = \frac{Sup({}^{\alpha}x_{\oplus,t+1})}{Sup(m_{1:t-1}) + Sup({}^{\alpha}x_{\oplus,t}) + Sup({}^{\alpha}x_{\oplus,t+1})} \tag{30} $$

$$ \begin{cases} \tau_t = Crd(m_{1:t-1}) + Crd(m_{1:t+1}),\ v_t = Crd({}^{\alpha}x_{\oplus,t}), \\ Sim(m_{1:t-1}, {}^{\alpha}x_{\oplus,t+1} \ge Sim({}^{\alpha}x_{\oplus,t}, {}^{\alpha}x_{\oplus,t+1})) \\ \tau_t = Crd(m_{1:t-1}),\ v_t = Crd({}^{\alpha}x_{\oplus,t}) + Crd({}^{\alpha}x_{\oplus,t+1}), \\ others \end{cases} \tag{31} $$

Step 3: Compare the similarity of $Sim(x_{1,t-1}, {}^{\alpha}x_{\oplus,t+1})$ and $Sim({}^{\alpha}x_{\oplus,t}, {}^{\alpha}x_{\oplus,t+1})$ to obtain $\{v_t, \tau_t\}$.

Remark 1: a is an adjustable parameter, which can adjust the influence for the difference of x_1, x_2. In addition, they are satisfied with (a) $Sim(x_1, x_1) = 1$; (b) $Sim(x_1, x_2) = Sim(x_2, x_1)$; (c) when $x_1 \neq x_2$, $Sim(x_1, x_1) > Sim(x_1, x_2)$ [37].

Remark 2: The updating combination weight $\{v_t, \tau_t\}$ will be defined in the same format as the adjustable parameter a. The $\{v_t, \tau_t\}$ will be optimized with the optimization of parameter a. In other words, the updated evidence for the reliability of the real failure value tends to be 1. The detailed construction description of a will be presented in the next part.

Remark 3: Combination weight $\{v_t, \tau_t\}$ can be adjusted adaptively via $Crd({}^{\alpha}x_{\oplus,t+1})$.

2) COMBINATION WEIGHT OPTIMIZATION

The fault credit dynamic convergence function is employed to optimize a, and then, the combination weight $\{v_t, \tau_t\}$ is also optimized.

Suppose T_l times fault feature samplings occur during the diagnosis process of No. $l(l = 1, 2, \cdots, L)$. After local evidence is obtained, static fusion, dynamic updating, and the global evidence $x_{1,t}(t = 1, 2, \cdots, T_l)$ will be obtained in turn. If there are $F^l_{T1}, F^l_{T2}, \cdots, F^l_{TM}$ operating states, then $F^l_{Tm} \in \{F_0, F_1, \cdots, F_n\}, m = 1, 2, \cdots, M$. Based on the diagnosis process and the corresponding global evidence sequence, the global evidence credit convergence objective function is defined by

$$\begin{aligned} UDI(a) = \frac{1}{L}\sum_{l=1}^{L}\Big(\frac{1}{M}\times\Big(\frac{1}{T_1}\sum_{t=1}^{T_1} sim(x_{1:t}, x_{F^l_{T1}}) \\ + \frac{1}{T_2}\sum_{t=T_1+1}^{T_1+T_2} sim(x_{1:t}, x_{F^l_{T2}}) + \cdots \\ + \frac{1}{T_M}\sum_{t=T_1+\cdots+T_{M-1}+1}^{T_1+\cdots+T_M} sim(x_{1:t}, x_{F^l_{TM}})\Big)\Big) \end{aligned} \tag{32}$$

where $x_{F^l_{Tx}} = x(F^l_{Tx}) = 1$ expresses the ideal reliability of the real fault status, T_x expresses the running times of No. M, and $\sum_{x=1}^{M} T_x = T_l$ expresses the sum of every diagnosis sample frequency. $\frac{1}{L}$, $\frac{1}{M}$ and $\frac{1}{T_x}$ express the normalization factor of the batch process, batch status and batch continuous status of diagnosis, respectively. $UDI = [0, 1]$ is guaranteed. The value of UDI is in direct proportion to the global evidence credit.

Considering the responding ability for the fault state, the adjacent moment global evidence credit convergence objective function is defined by

$$\begin{aligned} DDI(a) = \frac{1}{L}\sum_{l=1}^{L}\Big(\frac{1}{M}\times\Big(\frac{1}{T_1}\sum_{t=1}^{T_1}\lambda^l_{t,1}\Delta^l_{t,1} \\ + \frac{1}{T_2}\sum_{t=T_1+1}^{T_1+T_2}\lambda^l_{t,2}\Delta^l_{t,2} \\ + \cdots + \frac{1}{T_M}\sum_{t=T_1+\cdots+T_{M-1}+1}^{T_1+\cdots+T_M}\lambda^l_{t,M}\Delta^l_{t,M}\Big)\Big) \end{aligned} \tag{33}$$

where $\Delta^l_{t,x} = Sim\left(x_{1:t}, x_{F^l_{Tx}}\right) - Sim\left(x_{1:t-1}, x_{F^l_{Tx}}\right)$ expresses the difference value between $x_{1:t-1}$ and $x_{F^l_{Tx}}$. $\lambda^l_{t,m}$ expresses the fading factor of the tracking velocity and is defined by

$$\lambda^l_{t,m} = \begin{cases} \dfrac{1}{t} & m = 1, \quad t \geq 1 \\ \dfrac{1}{t - \sum_{j=1}^{m-1} T}, & 2 \leq m \leq M, \quad T_1 + 1 \leq t \leq \sum_{j=1}^{M} T_m \end{cases} \tag{34}$$

Remark 4: $DDI \in [-1, 1]$ and $DDI = 0$ indicate that $m_{1:t}$ has no ability to track the actual state of the satellite attitude, and $DDI > 0$ indicates that $m_{1:t}$ has the ability to track the actual state; otherwise, the wrong state is obtained by $m_{1:t}$. Regardless of whether $DDI > 0$ or $DDI < 0$, as long as the absolute value is higher, the tracing velocity is faster.

Considering the merits of both UDI and DDI, the dynamic convergence function of fault information can be defined by

$$DI(a) = \kappa \times (1 - UDI(a)) + \eta \times (1 - DDI(a)) \tag{35}$$

where κ, η are the weights of UDI and DDI, respectively, and $\kappa + \eta = 1, 0 \leq \kappa, \eta \leq 1$. UDI measures the responding ability of global evidence to an actual fault, and DDI measures the responding ability of updated process to change the fault state. Thus, the optimal parameter a and $\{v_t, \tau_t\}$ can be solved by the optimal model based on Eq.(35) as follows:

$$\begin{aligned} &\min_{a} DI(a) \\ &s.t.\ 0 \leq a \leq 50 \end{aligned} \tag{36}$$

IV. SIMULATION RESULTS

To demonstrate the effectiveness of the presented fault diagnosis method, an example of a rigid satellite is considered for numerical simulation. The principal moments of inertia of the considered satellite are $J_{11} = 45$ kgm^2, $J_{22} = 50$ kgm^2, and $J_{33} = 47.5$ kgm^2. The inertia products are smaller than 0.5 kgm^2. To illustrate the circumstance, such as external disturbance torque, $\boldsymbol{d}$ is assumed as follows:

$$\boldsymbol{d} = \begin{bmatrix} 5\cos(0.2\pi t) \\ -3\cos(0.2\pi t) \\ 2\cos(0.2\pi t) \end{bmatrix} \times 10^{-3} \tag{37}$$

In our simulation, the initial conditions of quaternion and angular velocity are $\sigma(0) = [\,0.288\ -0.143\ -0.020\,]^{\mathrm{T}}$ and $\omega(0) = [\,-1\ 0.8\ 0.4\,]^{\mathrm{T}}$ rad/sec, respectively. The parameters for the controller are chosen as $\alpha_1 = 1.2$, $\alpha_2 = 0.6$, $\beta_1 = 2.5$, $\gamma_1 = 0.8$, $\gamma_2 = 0.38$, $\varepsilon_0 = 0.75$, and $K = 0.15$. The parameters for the semi-supervision fault diagnosis should be satisfied with these rulers: 1) basic confidence value is greater than $a = 0.5$, 2) uncertainty $x(\Theta)$ is less than $b = 0.3$, and 3) the difference between BBA and out of BBA is not less than $c = 0.15$.

A. ACTUATOR UNCERTAINTIES

To investigate the proposed semi-supervision fault diagnosis performance, actuator uncertainties are considered. The following fault scenarios and misalignments are introduced:

- When the actuator is switched-on, a random misalignment corresponding to the thrust misalignment is considered. In such a case, this misalignment model is a Gaussian noise on both the azimuth and the elevation angles (*i.e.*, $\Delta\alpha_i$ and $\Delta\beta_i$, respectively) with standard deviation of 2.5% for each.
- Supplementary position of actuator Δr_i, $i = 1, 2, 3$ is a Gaussian noise model with the standard deviation is 4% for each.
- The fairly severe fault cases, shown in Fig. 5, are considered as follows:

Case 1, the actuator loses its power 50% of its normal value after t = 10 s.

Case 2, the actuator undergoes its loss power of 60% between the time interval from t = 5 s to t = 30 s, and an increased bias torque of 0.04 Nm occurred after t = 40 s.

Case 3, the actuator effectiveness decreases 40% of its normal value from t = 25 s to t = 50 s, and an increased bias torque 0.03 Nm occurred after t = 75 s.

The abovementioned faults are shown in the right plot of Fig. 5. Usually, a good fault monitoring and diagnosis step is the most important step for fault tolerance controller design. To clarify Fig. 5, note the following: Dot line part implies actuator normal, Horizontal line implies partial loss of effectiveness fault and Vertical line implies bias torque fault.

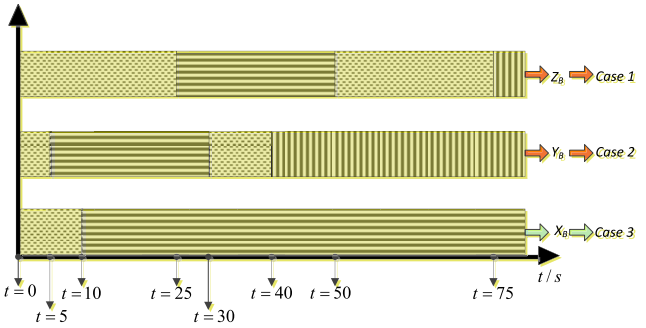

FIGURE 5. Three reaction wheels' fault scenarios.

B. FAULT DIAGNOSIS PERFORMANCE

Here, the method to obtain fault diagnosis evidence is from [2]. The local diagnosis evidence of every sampling time is from $\Delta F_1 \sim \Delta F_3$ and d (which are recorded $x_{1,t} - x_{4,t}$). The results $x_{\Theta,t}$ of static fusion are confirmed based the static fusion and dynamic updating, and then, the global pieces of evidence $x_{2,t}$ are obtained based on $x_{\Theta,t}$. During the simulation part, data samples are taken 30 times, 40 sets of data are obtained every time, and every set includes 4 data points. During this testing, data samplings are adopted to be training samplings 20 times, and the other 10 times, data samplings are adopted to be testing samplings.

To prove the excellent performance of the proposed semi-supervision fault diagnosis method, here, static fusion alone, dynamic updating alone and combined static fusion with dynamic updating are all employed in the following tests.

TABLE 1. Fault diagnosis based on lonely static fusion.

Decision results / Actual status	ΔF_1	ΔF_2	ΔF_3	d	Number of status	Accuracy
ΔF_1	380	25	68	0	473	80.51%
ΔF_2	0	198	21	15	234	81.14%
ΔF_3	4	2	150	21	177	84.29%
d	0	12	19	58	89	83.92%

TABLE 2. Fault diagnosis based on lonely dynamic updating.

Decision results / Actual status	ΔF_1	ΔF_2	ΔF_3	d	Number of status	Accuracy
ΔF_1	356	36	81	0	473	90.21%
ΔF_2	0	179	29	26	234	91.04%
ΔF_3	10	3	136	28	177	94.95%
d	0	16	20	53	89	93.21%

TABLE 3. *DDI*, *DI* values of ${}^{\alpha}x_{1,t}$.

Updated method	*DDI*	*DI* ($\eta = \kappa = 0.5$)
${}^{\alpha}x_{1,t}$	0.9631	0.0499

TABLE 4. Fault diagnosis based on semi-supervision fault diagnosis.

Decision results / Actual status	ΔF_1	ΔF_2	ΔF_3	d	Number of status	Accuracy
ΔF_1	354	35	84	0	473	95.68%
ΔF_2	0	175	31	29	234	97.12%
ΔF_3	8	3	139	27	177	95.39%
d	0	15	23	51	89	96.33%

Table 1 presents the fault diagnosis results based on static fusion alone. The diagnosis method includes two steps: first, using the fault feature data from the 20 times data sampling to form local pieces of evidence $x_{1,t} \sim x_{4,t}$, and second, using Eq.(19) to determine the optimal discount coefficient. Thus, the discount coefficient vector is defined as $\alpha_1 = (0, 0, 0.1959, 0.2601)$, $\alpha_2 = (0.0625, 0, 0, 0)$, $\alpha_3 = (0, 0, 0.0119, 0.9999)$, $\alpha_4 = (0, 0.0049, 0.1605, 0.0002)$. In addition, ${}^{\alpha}x_{\oplus,t} = 21.8905$ according to Eq.(18). Table 2 presents the fault diagnosis results based on dynamic updating alone. To solve the optimal solution of Eq.(36), obtain the parameter a of S similar function, and then, update the corresponding optimal weight $\{\tau_t, v_t\}$. In the testing, we set $a = 25$. Eq.(31) is used to calculate $\{\tau_t, v_t\}$, and then, the updated pieces of evidence ${}^{\alpha}x_{\oplus,t}$ are obtained. Here, we set the next moment updated evidence as ${}^{\alpha}x_{1,t}$. The index values of *DDI*, *DI* are presented in Table 3. To prove the high fault diagnosis accuracy, Table 4 presents the fault diagnosis based

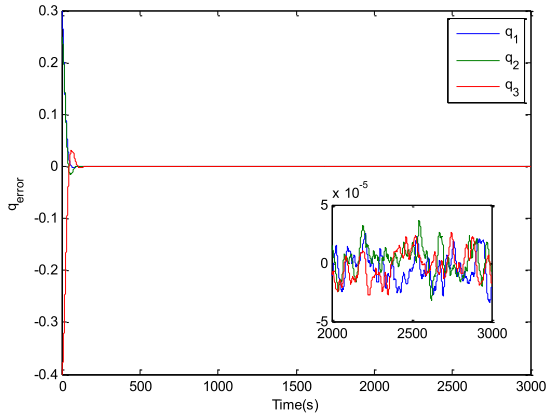

FIGURE 6. Fault diagnosis error of q without actuator faults; the left plot shows results of the whole fault diagnosis error (delay-time is considered, and the right plot shows the fault diagnosis error after steady state is achieved).

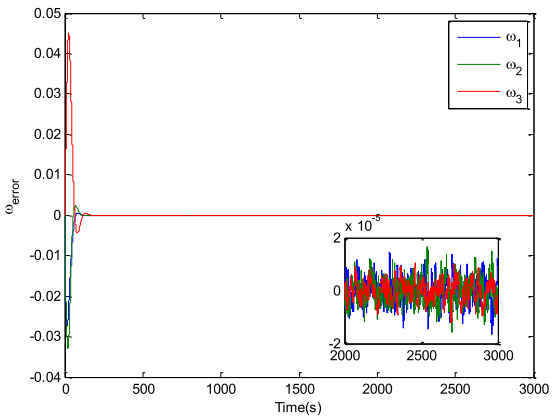

FIGURE 7. Fault diagnosis error of ω without actuator faults; the left plot shows results of the whole fault diagnosis error (delay-time is considered, and the right plot shows the fault diagnosis error after steady state is achieved).

on semi-supervision fault diagnosis. The method combined static fusion with dynamic updating.

From Tables 1, 2, and 4, we can find that Table 4 has the higher accuracy than Tables 1-2. In other words, the combination of static fusion and dynamic updating can bring more merit to the accuracy of fault diagnosis. To show the fault diagnosis accuracy, fault diagnosis error information is employed here.

The fault diagnosis error $\boldsymbol{e}$ (denoted as $\boldsymbol{\omega}$, $\boldsymbol{q}$ and $\boldsymbol{u}$) between the actual fault states and their estimates fault states are shown in Fig. 6-11. The precisely fault diagnosis information of the actuator faults and external disturbances will give a strong support for a good fault tolerance controller, especially for rejecting external disturbances and the other uncertainty of actuators completely. Therefore, accurate fault diagnosis is essential.

Figs. 6-8 show the fault diagnosis error states when all the actuators are normal. The fault diagnosis results are shown clearly via $\boldsymbol{e} = 0$ or $\boldsymbol{e} \to 0$. In addition, Figs. 9-11 show

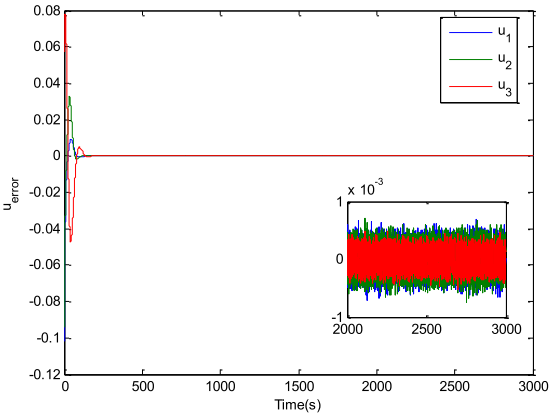

FIGURE 8. Fault diagnosis error of u without actuator faults; the left plot shows results of the whole fault diagnosis error (delay-time is considered, and the right plot shows the fault diagnosis error after steady state is achieved).

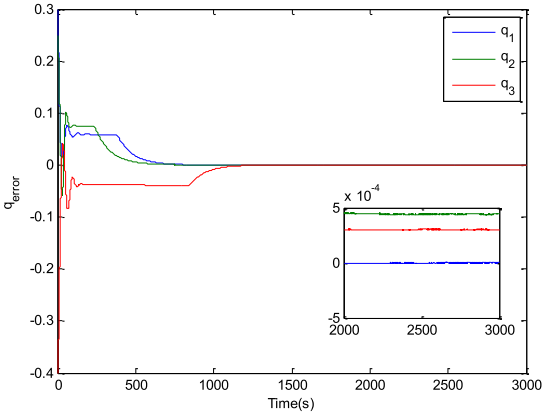

FIGURE 9. Fault diagnosis error of q with actuator faults; the left plot shows results of the whole fault diagnosis error (delay-time is considered, and the right plot shows the fault diagnosis error after steady state is achieved).

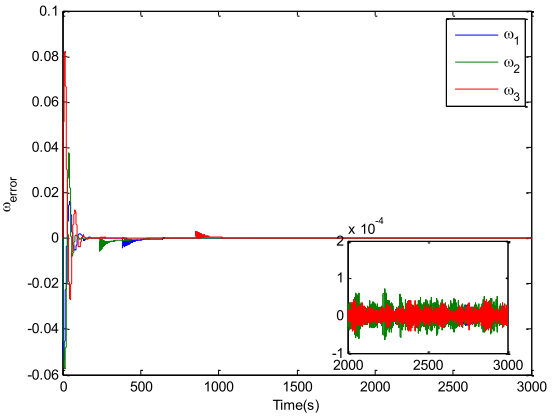

FIGURE 10. Fault diagnosis error of ω with actuator faults; the left plot shows results of the whole fault diagnosis error (delay-time is considered, and the right plot shows the fault diagnosis error after steady state is achieved).

$\boldsymbol{e} \to 0$ with the fault Cases 1-3. The conclusion can be drawn that the semi-supervision fault diagnosis method has good fault diagnosis ability.

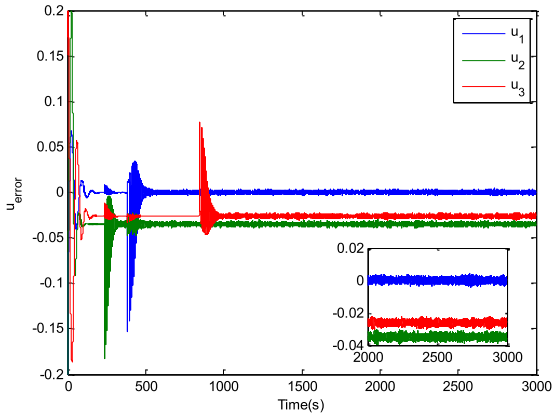

FIGURE 11. Fault diagnosis error of u with actuator faults; the left plot shows results of the whole fault diagnosis error (delay-time is considered, and the right plot shows the fault diagnosis error after steady state is achieved).

V. CONCLUSION

A semi-supervision fault diagnosis method based on attitude information for a satellite is proposed. This method combines static fusion with dynamic updating. It not only detects the slow change and failure with interference but also confirms the optimal fusion and updated parameters based on the historical data. The fault diagnosis designs are evaluated using numerical simulation to compare and prove the effectiveness of the proposed method.

REFERENCES

[1] D. van Schrick, "Remarks on terminology in the field of supervision, fault detection and diagnosis," *IFAC Proc. Volumes*, vol. 30, no. 18, pp. 959–964, 1997.

[2] Z. Gao, C. Cecati, and S. X. Ding, "A survey of fault diagnosis and fault-tolerant techniques—Part I: Fault diagnosis with model-based and signal-based approaches," *IEEE Trans. Ind. Electron.*, vol. 62, no. 6, pp. 3757–3767, Jun. 2015.

[3] Z. Gao, C. Cecati, and S. X. Ding, "A survey of fault diagnosis and fault-tolerant techniques—Part II: Fault diagnosis with knowledge-based and hybrid/active approaches," *IEEE Trans. Ind. Electron.*, vol. 62, no. 6, pp. 3768–3774, Jun. 2015.

[4] R. Isermann, "Process fault detection based on modeling and estimation methods—A survey," *Automatica*, vol. 20, no. 4, pp. 387–404, 1984.

[5] P. M. Frank, "Fault diagnosis in dynamic systems using analytical and knowledge-based redundancy: A survey and some new results," *Automatica*, vol. 26, no. 3, pp. 459–474, 1990.

[6] E. A. García and P. M. Frank, "Deterministic nonlinear observer-based approaches to fault diagnosis: A survey," *Control Eng. Pract.*, vol. 5, no. 5, pp. 663–670, 1997.

[7] R. Isermann and P. Ballé, "Trends in the application of model-based fault detection and diagnosis of technical processes," *Control Eng. Pract.*, vol. 5, no. 5, pp. 709–719, 1997.

[8] P. M. Frank and X. Ding, "Survey of robust residual generation and evaluation methods in observer-based fault detection systems," *J. Process Control*, vol. 7, no. 6, pp. 403–424, 1997.

[9] R. Isermann, "Model-based fault-detection and diagnosis—Status and applications," *Annu. Rev. Control*, vol. 29, no. 1, pp. 71–85, 2005.

[10] X. Zhao, P. Shi, and X. Zheng, "Fuzzy adaptive control design and discretization for a class of nonlinear uncertain systems," *IEEE Trans. Cybern.*, vol. 46, no. 6, pp. 1476–1483, Jun. 2015.

[11] X. Zhao, H. Yang, H. R. Karimi, and Y. Zhu, "Adaptive neural control of MIMO nonstrict-feedback nonlinear systems with time delay," *IEEE Trans. Cybern.*, vol. 46, no. 6, pp. 1337–1349, Jun. 2016.

[12] S. Yin, H. Yang, and O. Kaynak, "Sliding mode observer-based FTC for Markovian jump systems with actuator and sensor faults," *IEEE Trans. Autom. Control*, vol. 62, no. 7, pp. 3551–3558, Jul. 2017.

[13] S. Yin, H. Gao, J. Qiu, and K. Kaynak, "Descriptor reduced-order sliding mode observers design for switched systems with sensor and actuator faults," *Automatica*, vol. 76, pp. 282–292, Feb. 2017.

[14] V. Venkatasubramanian, R. Rengaswamy, and S. N. Kavuri, "A review of process fault detection and diagnosis: Part II: Qualitative models and search strategies," *Comput. Chem. Eng.*, vol. 27, no. 3, pp. 313–326, 2003.

[15] V. Venkatasubramanian, R. Rengaswamy, S. N. Kavuri, and K. Yin, "A review of process fault detection and diagnosis: Part I: Quantitative model-based methods," *Comput. Chem. Eng.*, vol. 27, no. 3, pp. 293–311, 2003.

[16] V. Venkatasubramanian, R. Rengaswamy, S. N. Kavuri, and K. Yin, "A review of process fault detection and diagnosis: Part III: Process history based methods," *Comput. Chem. Eng.*, vol. 27, no. 3, pp. 327–346, 2003.

[17] Q. Wu and R. Law, *Complex System Fault Diagnosis Based on a Fuzzy Robust Wavelet Support Vector Classifier and an Adaptive Gaussian Particle Swarm Optimization*. New York, NY, USA: Elsevier, 2010.

[18] S. Yin, X. Zhu, and C. Jing, "Fault detection based on a robust one class support vector machine," *Neurocomputing*, vol. 145, pp. 263–268, Dec. 2014.

[19] X. Xie, W. Sun, and K. C. Cheung, "An advanced PLS approach for key performance indicator-related prediction and diagnosis in case of outliers," *IEEE Trans. Ind. Electron.*, vol. 63, no. 4, pp. 2587–2594, Apr. 2016.

[20] S. Yin, X. Zhu, and O. Kaynak, "Improved PLS focused on key-performance-indicator-related fault diagnosis," *IEEE Trans. Ind. Electron.*, vol. 62, no. 3, pp. 1651–1658, Mar. 2015.

[21] D. Goodhue, W. Lewis, and R. Thompson, "Research note—Statistical power in analyzing interaction effects: Questioning the advantage of PLS with product indicators ," *Inf. Syst. Res.*, vol. 18, no. 2, pp. 211–227, 2007.

[22] C. Angeli and A. Chatzinikolaou, "On-line fault detection techniques for technical systems: A survey," *Int. J. Comput. Sci. Appl.*, vol. 1, no. 1, pp. 12–30, 2004.

[23] X. Dai and Z. Gao, "From model, signal to knowledge: A data-driven perspective of fault detection and diagnosis," *IEEE Trans. Ind. Informat.*, vol. 9, no. 4, pp. 2226–2238, Nov. 2013.

[24] S. Yin, S. X. Ding, X. Xie, and H. Luo, "A review on basic data-driven approaches for industrial process monitoring," *IEEE Trans. Ind. Electron.*, vol. 61, no. 11, pp. 6418–6428, Nov. 2014.

[25] G. Wang, S. Yin, and O. Kaynak, "An LWPR-based data-driven fault detection approach for nonlinear process monitoring," *IEEE Trans. Ind. Informat.*, vol. 10, no. 4, pp. 2016–2023, Nov. 2014.

[26] R. Isermann, "Supervision, fault-detection and fault-diagnosis methods—An introduction," *Control Eng. Pract.*, vol. 5, no. 5, pp. 639–652, 1999.

[27] P. Bojanowski and A. Joulin. (Apr. 2017). "Unsupervised learning by predicting noise." [Online]. Available: https://arxiv.org/abs/1704.05310

[28] E. Shutova, L. Sun, E. D. Gutiérrez, P. Lichtenstein, and S. Narayanan, "Multilingual metaphor processing: Experiments with semi-supervised and unsupervised learning," *Comput. Linguistics*, vol. 43, no. 1, pp. 71–123, 2017.

[29] B. Li, Q. Hu, Y. Yu, and G. Ma, "Fault tolerant attitude control for rigid spacecraft," *IEEE Trans. Aerosp. Electron. Syst.*, vol. 43, no. 5, pp. 2644–2663, May 2017.

[30] M. J. Sidi, *Spacecraft Dynamics and Control*. Cambridge, U.K.: Cambridge Univ. Press, 1997.

[31] A. Valdes and K. Khorasani, "A pulsed plasma thruster fault detection and isolation strategy for formation flying of satellites," *Appl. Soft Comput.*, vol. 10, no. 3, pp. 746–758, Jun. 2010.

[32] X. Xiaobin *et al.*, "Fault diagnosis based on fusion and updating of diagnosis evidence," *Acta Autom. Sinica*, vol. 42, pp. 107–121, Jan. 2016.

[33] D. Mercier, B. Quost, and T. Denæux, "Refined modeling of sensor reliability in the belief function framework using contextual discounting," *Inf. Fusion*, vol. 9, no. 2, pp. 246–258, 2008.

[34] P. Smets, "About updating," in *Proc. 7th Conf. Uncertainty Artif. Intell.*, 1991, pp. 378–385.

[35] E. C. Kulasekere, K. Premaratne, D. A. Dewasurendra, M.-L. Shyu, and P. H. Bauer, "Conditioning and updating evidence," *Int. J. Approx. Reasoning*, vol. 36, no. 1, pp. 75–108, 2004.

[36] H. Guo, W. Shi, and Y. Deng, "Evaluating sensor reliability in classification problems based on evidence theory," *IEEE Trans. Syst., Man, Cybern. B, Cybern.*, vol. 36, no. 5, pp. 970–981, Oct. 2006.

[37] A. L. Jousselme, D. Grenier, and É. Bossé, "A new distance between two bodies of evidence," *Inf. Fusion*, vol. 2, no. 2, pp. 91–101, 2001.

ZHIQIANG ZHANG received the B.S. degree from Jinzhou Teacher's College in 2000 and the M.S. degree from Dalian University of Technology in 2008. He is currently an Associate Professor at Bohai University. His current research interests include machine learning and pattern recognition.

ZHIYONG SHE received the B.S., M.S., and Ph.D. degrees from Harbin Institute of Technology in 2004, 2006, and 2010, respectively. He is currently a Professor at Bohai University. His current research interests include fault diagnosis, fault tolerance, and attitude control of satellites.

AIHUA ZHANG received the B.S. and M.S. degrees from Jinzhou Teacher's College in 2000 and 2008, respectively, and the Ph.D. degree from Harbin Institute of Technology in 2014. She is currently a Professor at Bohai University. Her current research interests include fault diagnosis, fault tolerance, and attitude control of satellites.